The Limiting Role of Iodide Oxidation in *cis*-Os(dcb)$_2$(CN)$_2$/TiO$_2$ Photoelectrochemical Cells

Monica Alebbi and Carlo A. Bignozzi*

Dipartimento di Chimica dell'Universita, Centro di Studio su Fotoreattivita e Catalisi CNR, 44100 Ferrara, Italy

Todd A. Heimer, Georg M. Hasselmann, and Gerald J. Meyer*

Department of Chemistry, Johns Hopkins University, Baltimore, Maryland 21218

Received: March 26, 1998; In Final Form: July 20, 1998

Porous nanostructured photoanodes prepared from colloidal solutions of DeGussa or sol−gel processed TiO$_2$ material have been derivatized with *cis*-M(dcb)$_2$(CN)$_2$, where M = Ru(II) or Os(II) and dcb is 4,4′-(COOH)$_2$-2,2′-bipyridine. When employed in a regenerative solar cell with iodide donors, *cis*-Ru(dcb)$_2$(CN)$_2$/TiO$_2$ converts absorbed photons to electrons nearly quantitatively while *cis*-Os(dcb)$_2$(CN)$_2$/TiO$_2$ does not. In-situ time-resolved diffuse reflectance measurements reveal a sluggish iodide oxidation rate is responsible for the low photocurrent efficiency of *cis*-Os(dcb)$_2$(CN)$_2$/TiO$_2$. Transient absorption measurements support this conclusion and allow full wavelength characterization of the charge-transfer processes.

Introduction

Dye-sensitized wide-band-gap semiconductor materials provides an excellent opportunity to probe interfacial electron-transfer dynamics at the molecular level.[1] High-surface-area nanocrystalline semiconductor films yield remarkably high light-to-electrical energy conversion efficiencies and also allow electron-transfer processes to be spectroscopically and electrochemically quantified.[2] Systematic studies have provided,[1] and continue to provide, fundamental insights into the light-to-electrical conversion mechanism(s).[3] Furthermore, energy wasting recombination processes have been identified that are becoming more fully understood.[4]

This manuscript is a follow-up to previous work where it was noted that *cis*-Ru(dcb)$_2$(CN)$_2$ (dcb is 4,4′-(COOH)$_2$-2,2′-bipyridine) converts photons into electrons quantitatively while *cis*-Os(dcb)$_2$(CN)$_2$ did not.[5] The observation was disappointing since Os(II) complexes are known to be more photochemically robust than analogous Ru(II) complexes and may, therefore, be better suited for practical applications in solar cells.[6] The dissimilar photoelectrochemical behavior was rationalized in terms of sensitizer photophysical and redox properties measured in fluid aqueous solution. Using this approach, a crude energy level diagram was constructed at pH 2 (Scheme 1, potentials vs SSCE). The energetic coincidence of the excited-state potentials, long nanosecond lifetimes, and related reports in the literature led to the assumption that the quantum yield for electron injection was the same for these two closely related sensitizers.[5] In light of recent ultrafast electron injection reports, this assumption appears even more reasonable today.[7] Furthermore, the sensitizers have comparable extinction coefficients, and photoelectrochemical measurements demonstrated that the differences in photocurrent efficiency was not simply due to the amount of incident light absorbed.[5]

A key difference between the sensitizers is their ground-state oxidation potentials, Scheme 1. The 340 mV difference between the Os$^{III/II}$ and Ru$^{III/II}$ redox couples couple could manifest itself in different halide oxidation rates (k_4) and/or recombination rates with the electron in the solid (k_3), either of which is expected to significantly effect the photon-to-current efficiency.[3] In previous photoelectrochemical studies, the limiting role of halide oxidation on the observed photocurrent in stirred and unstirred electrolyte solutions with iodide or bromide was noted.[5] Furthermore, we noted that Marcus theory for nonadiabatic electron transfer in the inverted kinetic region is consistent with a faster recombination rate for surface-anchored *cis*-Os(dcb)$_2$-(CN)$_2$.[5] However, photoelectrochemical measurements and solution redox potentials alone were unable to conclusively determine the origin of the lower photocurrent for the Os sensitizer.

SCHEME 1

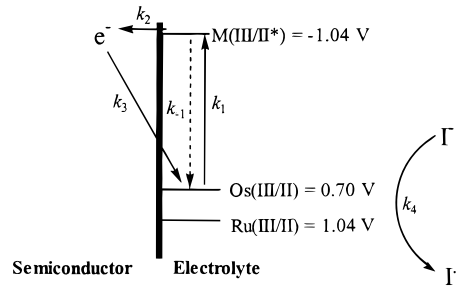

Here we present time-resolved absorption and diffuse reflectance measurements of these same sensitizers anchored to related TiO$_2$ materials in regenerative photoelectrochemical cells. These experiments allow the relative roles of charge recombination and iodide oxidation to be quantitatively assessed. The results indicate that the lower photocurrent efficiency observed for *cis*-Os(dcb)$_2$(CN)$_2$ is due to a sluggish iodide oxidation rate. We note that a preliminary account of the diffuse reflectance studies was recently reported.[8]

Experimental Section

Materials. All reagents were of the highest purity commercially available and were used without further purification.

Sensitizer Preparation. The sensitizers were prepared and characterized as previously described.[5] The ^{1}H NMR were not reported previously and are therefore given here.

Na$_4$[Ru(4,4′-(CO$_2^-$)$_2$-2,2′-bipyridine)$_2$(CN)$_2$]: D$_2$O; δ = 9.37 ppm (d, 2 H, 6), 8.64 (s, 2 H, 3), 8.55 (s, 2 H, 3′), 7.83 (d, 2 H, 5), 7.53 (d, 2 H, 6′), 7.38 (d,2 H, 5′).

S1089-5647(98)01643-5 CCC: $15.00
Published on Web 09/09/1998

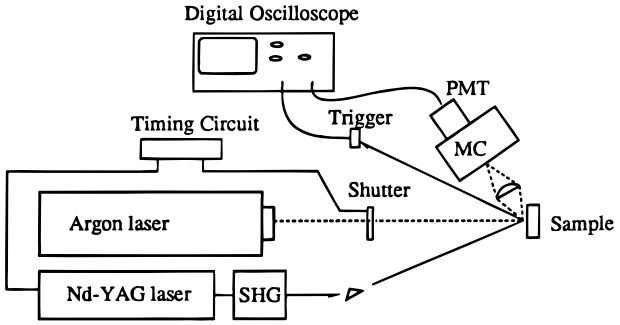

Figure 1. Schematic representation of the time-resolved diffuse reflectance apparatus. The probe light was the 488-nm line from the argon ion laser and the excitation source was the 532-nm line from the Nd:YAG laser. The instrument response function of the apparatus is ~15 ns.

$Na_4[Os(4,4'\text{-}(CO_2^-)_2\text{-}2,2'\text{-bipyridine})_2(CN)_2]$: D_2O; δ = 9.49 ppm (d, 2 H, 6), 8.63 (s, 2 H, 3), 8.54 (s, 2 H, 3′), 7.75 (d, 2 H, 5), 7.49 (d, 2 H, 6′), 7.33 (d,2 H, 5′).

Materials Preparation. Preparation of the nanostructured TiO_2 electrodes from an aqueous suspension of Degussa P25 TiO_2 has been previously described.[9] The Degussa material is comprised of approximately 70% anatase and 30% rutile and was used for photoelectrochemical and diffuse reflectance measurements. The preparation of sol−gel processed anatase TiO_2 films with high optical transparency have also been previously reported.[10] The sol−gel processed material is comprised of ~20-nm anatase particles and was used for photoelectrochemical and transient absorption measurements. Attachment of the sensitizer molecule to the films is achieved by soaking the TiO_2 electrode in $\cong 1 \times 10^{-4}$ M ethanol or acetonitrile solutions of the dye for 24 h. Surface coverage of the sensitizer is estimated by the change in absorbance of the solution after soaking.

Regenerative Cell Assembly. The sensitized electrode is coated with an electrolytic solution of 0.5 M NaI and 0.05 M I_2 in acetonitrile or propylene carbonate. The cell is then assembled by placing the electrode against a second fluorine-doped tin oxide electrode onto which a thin coat of platinum had been sputtered. The two electrodes are held together using a spring clamp. All experiments were performed in this regenerative "sandwich" cell arrangement. The geometric electroactive area of these cells was typically 1 cm^2.

Photoelectrochemical Measurements. Incident photon-to-current conversion efficiency (IPCE) was measured in the regenerative cell assembly described above, and calculated as previously described.[5] The cell was excited through the dye-coated photoanode with a 150-W Xe lamp coupled to an *f*/2 McPherson monochromator equipped with a holographic grating and a 3.2-mm fiber optic bundle. Current measurements were performed using a Keithley model 617 digital electrometer having an input voltage burden of less than 3 mV. Incident irradiance was measured with a calibrated silicon photodiode obtained from UDT Technologies.

Diffuse Reflectance. The experimental arrangement for diffuse reflectance, shown in Figure 1, was similar to that described by Wilkinson.[11b] The attenuated 488-nm line of a coherent Ar^+ laser served as the probe beam, incident perpendicular to the sandwich cell. The diffuse reflected light was coupled to an *f*/3.4 monochromator equipped with an R928 photomultiplier tube. Excitation of the sample was provided by 8−10-ns fwhm 532-nm pulses from a Surelite I Nd:YAG laser. The transient diffuse reflectance absorption data are presented in the form of ΔJ, as a function of time, eq 1. In this expression, J_0 represents the reflectance of the sample prior

$$\Delta J(t) = \frac{J_0(t) - J_t(t)}{J_0(t)} \quad (1)$$

to excitation; J_t is the reflectance at time t following excitation.[11] The data presented have been normalized.

The kinetic analysis of diffuse reflectance data is not straightforward since ΔJ has no direct connection to basic transient properties. Traditionally, Kubelka−Munk theory has been proven to hold for many opaque diffuse reflectors.[11] We have used the simplified percent absorption calculation of Draper and Fox to analyze our data.[12] An underlying assumption of this method is that the initial transient concentration is proportional to the excitation irradiance. This requires that the signal height, ΔJ, at an arbitrary time following the excitation pulse be linearly proportional to the transient concentration over the range of excitation irradiance used for the kinetic experiments. We found ΔJ (t = 100 ns) to be linear with pump irradiances from 2.8 to 17.7 mJ/pulse; 100 ns was chosen as it is well outside the 15-ns instrument response function, yet the transient decays still have appreciable amplitude. Significant deviations from linearity were observed for irradiances exceeding 20 mJ/pulse. For the data presented here, experiments were performed at 12 ± 2 mJ/pulse. Once it is established that ΔJ is linearly proportional to transient concentration, standard kinetic analysis can be used.

Absorption. Nanosecond transient absorption measurements were performed with apparatus that has been previously described.[10] Briefly, excitation was carried out using the 532-nm laser pulses, ca. 8 ns and 20−25 mJ/pulse, from a Nd:YAG (Continuum Surelite). The approximately 5-mm diameter excitation beam was expanded to ca. 3 cm using a quartz plano-concave lens (JML Direct, −50 mm EFL, 25.4 mm diameter), resulting in a fluence of around 3 mJ cm^{-2}. The absorbance change of the laser-irradiated sample was probed at 90° to the excitation pulse using an Applied Photophysics 150-W Xe arc lamp operating in pulsed mode. The sample was protected from the probe light using a fast shutter, 10-ms pulse width, and appropriate UV and heat-absorbing glass and solution filter combinations. The probe light was focused onto the sample and again onto the entrance slit of a *f*/3.4 Applied Photophysics monochromator, typically under conditions such that the effective bandwidth was 2−3 nm. The probe beam was monitored after the monochromator using a Hamamatsu R928 photomultiplier. The instrument response function is 15 ns. Steady-state absorption measurements before and after transient measurements reveal no evidence of sensitizer decomposition.

Steady-state absorption measurements were made on a HP 8453 diode array spectrometer. For absorption measurements of sensitizers bound to nanocrystalline TiO_2 films, an underivatized film was used as the reference.

Results

Photoelectrochemistry. Shown in Figure 2 are the photoaction spectra of sol−gel processed TiO_2 films with surface anchored *cis*-$Ru(dcb)_2(CN)_2$ or *cis*-$Os(dcb)_2(CN)_2$ in acetonitrile electrolyte. The absorption spectra of these same two sensitizers are also given. Even though the osmium complex absorbs more light, it has a lower incident photon-to-current efficiency (IPCE) than does the ruthenium sensitizer. The same behavior is observed in propylene carbonate electrolyte and with sensitized DeGussa TiO_2 thin films. In all cases examined, when corrections were made for ground-state absorption, the IPCE

TABLE 1: Electron Transfer Kinetics for *cis*-M(dcb)$_2$(CN)$_2$/TiO$_2$ (M = Ru or Os)[a]

	diffuse reflectance[b]			transmission[c]		
sensitizer	$k_3 \times 10^6$ (s^{-1})	$k_{obs} \times 10^6$ (s^{-1})	$k_4 \times 10^7$ ($M^{-1}\ s^{-1}$)	$\langle k_3 \rangle \times 10^6$ (s^{-1})	$\langle k_{obs} \rangle \times 10^6$ (s^{-1})	$\langle k_4 \rangle \times 10^7$ ($M^{-1}\ s^{-1}$)
Ru(dcb)$_2$(CN)$_2$	3.5 ± 0.7	23 ± 5	2	2.0 ± 0.7	11 ± 6	2
Os(dcb)$_2$(CN)$_2$	4.5 ± 0.9	4.3 ± 0.6	< 0.9	3.3 ± 0.7	3.4 ± 0.6	< 0.7

[a] Kinetic rate constants abstracted from transient spectroscopic data measured in propylene carbonate electrolyte at room temperature. The notation corresponds to that shown in Scheme 1. See text for more details. [b] Reflectance transients observed at 488 nm in propylene carbonate electrolyte and fit to a single-exponential kinetic model. The errors represent one standard deviation from five separate samples sensitized electrodes prepared from DeGussa TiO$_2$ and measured under the same experimental conditions. [c] Absorption transients measured at the isosbestic wavelength between the excited state and ground state. The apparent first-order rate constants correspond to an average rate constant calculated from a biexponential fit to the observed transients. The errors represent one standard deviation from at least five separate sol−gel processed, sensitized TiO$_2$ electrodes prepared and measured under the same experimental conditions.

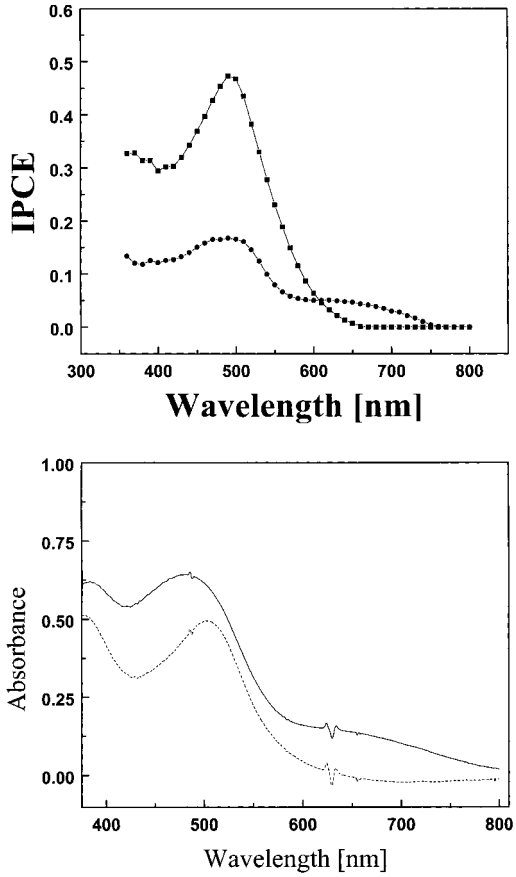

Figure 2. Upper panel: Photoaction spectrum of *cis*-Ru(dcb)$_2$(CN)$_2$ (squares) and *cis*-Os(dcb)$_2$(CN)$_2$ (circles) anchored to sol−gel processed TiO$_2$ thin films in 0.05 M I$_2$/ 0.5 M NaI acetonitrile solutions. IPCE is the incident photon-to-current efficiency. Lower panel: Absorption spectrum of the same electrodes in acetonitrile, *cis*-Ru(dcb)$_2$(CN)$_2$ (dashed line) and *cis*-Os(dcb)$_2$(CN)$_2$ (solid line).

of *cis*-Os(dcb)$_2$(CN)$_2$/TiO$_2$ was significantly lower than *cis*-Ru(dcb)$_2$(CN)$_2$/TiO$_2$.

Diffuse Reflectance. Shown in the Supporting Information are single wavelength (488 nm) time-resolved diffuse reflectance transients of *cis*-Ru(dcb)$_2$(CN)$_2$ and *cis*-Os(dcb)$_2$(CN)$_2$ anchored to DeGussa TiO$_2$ in a sandwich cell arrangement with a Pt counter electrode and propylene carbonate electrolyte. The initial decrease in reflectance cannot be resolved by this instrumentation. The magnitude of the reflectance signal was generally found to be the same for the two sensitizers within experimental error. The slow recovery occurs on a microsecond time scale and were found to be exponential with this poor signal-to-noise ratio. Table 1 summarizes the kinetics measured for five different sensitized electrodes prepared from DeGussa TiO$_2$. The apparent first-order rate constants abstracted for a large number of sensitized TiO$_2$ electrodes were within experimental error the same for both sensitizers. At this wavelength, these rates could reflect k_3, k_{-1}, or both. However, considering the high quantum yield for electron injection measured photoelectrochemically for *cis*-Ru(dcb)$_2$(CN)$_2$/TiO$_2$, and the relatively short excited-state lifetimes of these sensitizers, the transients shown should largely reflect the rate of electron tunneling from the semiconductor to the oxidized sensitizer, k_3 as discussed further below.

Addition of 0.5 M NaI to the cell assembly dramatically increases the rate of *cis*-Ru(dcb)$_2$(CN)$_2$/TiO$_2$ recovery but had no effect on the *cis*-Os(dcb)$_2$(CN)$_2$/TiO$_2$ kinetics within experimental error. Assuming this temporal change is due solely to sensitizer reduction by iodide, k_4 is calculated as the difference. For a large number of *cis*-Ru(dcb)$_2$(CN)$_2$/TiO$_2$ electrodes in 0.5 M NaI propylene carbonate, the estimated second-order rate constant is $k_4 = 2 \times 10^7\ M^{-1}\ s^{-1}$.

Excited-State Absorption Measurements. The preparation of optically transparent TiO$_2$ electrodes by sol−gel techniques and a white light probe beam allows transient absorbance measurements to be made throughout the visible region in a transmission mode. Absorption difference spectra are shown in Figure 3 for *cis*-Ru(dcb)$_2$(CN)$_2$/TiO$_2$ and *cis*-Os(dcb)$_2$(CN)$_2$/TiO$_2$ at the indicated delay times after pulsed excitation with green 532-nm light. No clear spectroscopic evidence for TiO$_2$(e$^-$) is observed under these conditions, and the difference spectra are assigned to the oxidized sensitizers.

For the data shown in Figure 3, the ground-state absorption at the excitation wavelength were 0.28 for *cis*-Os(dcb)$_2$(CN)$_2$/TiO$_2$ and 0.32 for *cis*-Ru(dcb)$_2$(CN)$_2$/TiO$_2$. Given that the extinction coefficients in the visible region are comparable,[5] that the laser irradiance was the same, and that the oxidized forms of these sensitizers are expected to absorb very little light in this region,[6] the comparable magnitude of the absorption bleach suggests comparable quantum yields for electron injection for these two sensitizers. Absolute actinometry is not possible in this system due to the instability of the oxidized *cis*-Ru(dcb)$_2$(CN)$_2$ which precludes spectroelectrochemical characterization. Nevertheless, relative actinometry for many samples consistently indicated that the quantum yields for electron injection were comparable, if not the same, for these two sensitizers.

Figure 4 displays absorption traces measured at 488 nm for *cis*-Ru(dcb)$_2$(CN)$_2$/TiO$_2$ and *cis*-Os(dcb)$_2$(CN)$_2$/TiO$_2$ under the same conditions as the diffuse reflectance measurements. The time scale of the decay is similar to that measured by transient diffuse reflectance spectroscopy. However, with improved S/N an absorption transient that extends to a tens of microsecond time scales is revealed. The transients do cleanly recover to baseline on a longer time scale that is shown and there is no evidence for sensitizer decomposition. The isosbestic points between the ground and excited state are $\lambda_{iso} = 415 \pm 5$ nm for

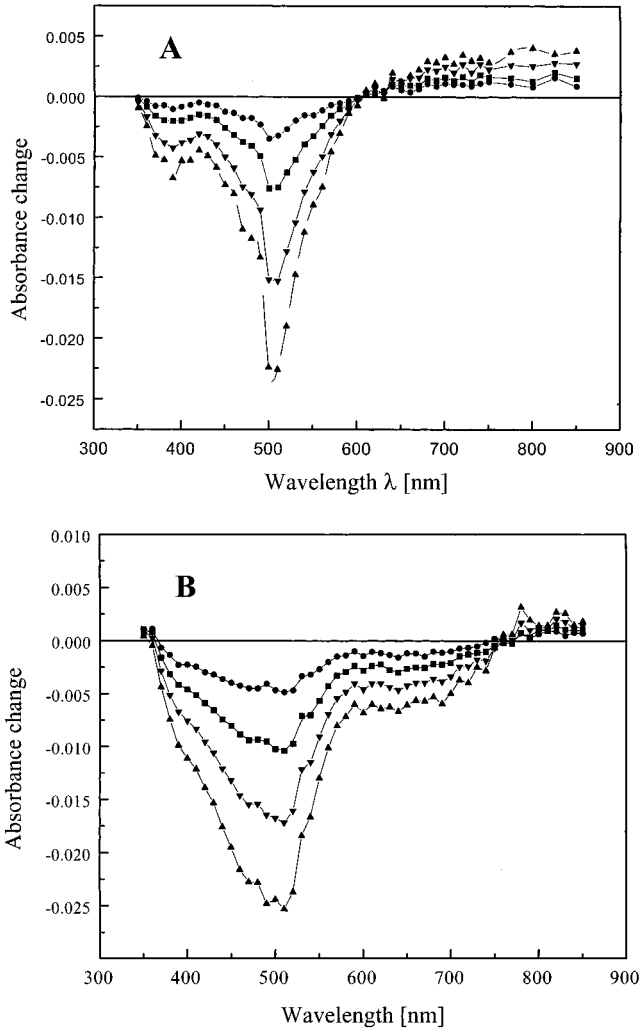

Figure 3. Absorbance difference spectra recorded for (A) *cis*-Ru(dcb)$_2$(CN)$_2$/TiO$_2$, 10, 50, 1000, and 5000 ns, and (B) *cis*-Os(dcb)$_2$(CN)$_2$/TiO$_2$, 10, 50, 200, and 1000 ns after a 532-nm light pulse (8−10 ns fwhm, 4 mJ/pulse) in 0.5 M LiClO$_4$/acetonitrile.

cis-Os(dcb)$_2$(CN)$_2$ and $\lambda_{iso} = 420 \pm 5$ nm for *cis*-Ru(dcb)$_2$(CN)$_2$ in propylene carbonate electrolyte. Absorption transients measured at this wavelength were analyzed in most detail to preclude possible contributions from unquenched excited states. However, the kinetics were found to be independent of the monitoring wavelength within experimental error which supports the assumption made for kinetic analysis of the diffuse reflectance data. Transients could not be fit to a single exponential but were fit to a sum of two exponentials, eq 2,

$$\Delta A(t) = \sum_{i=1}^{2} \alpha_i \exp(-k_i t) \qquad (2)$$

and an average rate constant was calculated as the first moment. The biexponential model is used solely to model the data. Rate constants abstracted should be viewed with caution and are best used for internal comparisons.[4] The addition of 0.5 M NaI results in a rapid recovery for the Ru(II) sensitizer that is well described by the biexponential model. The difference in average rate constants in the presence and absence of 0.5 M NaI is 9×10^6 s^{-1}, $\langle k_4 \rangle = 2 \times 10^7$ M^{-1} s^{-1} in good agreement with the diffuse reflectance data. No significant changes in the absorption transients are observed for the Os(II) sensitizer after addition of 0.5 M NaI indicating that $\langle k_4 \rangle < 7 \times 10^6$ M^{-1} s^{-1}, Figure 4.

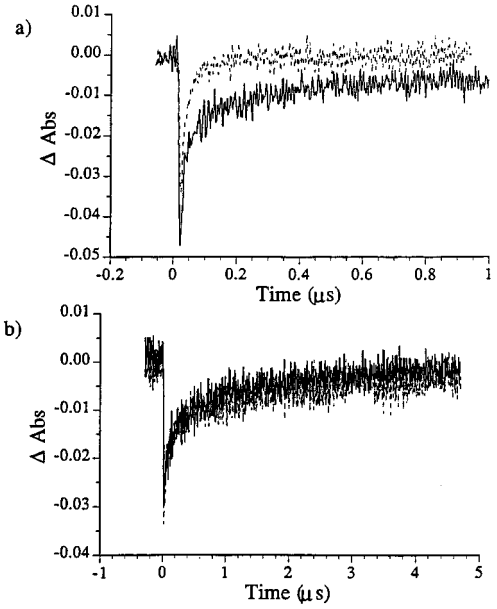

Figure 4. Single wavelength absorption transients for (a) *cis*-Ru(dcb)$_2$(CN)$_2$/TiO$_2$ and (b) *cis*-Os(dcb)$_2$(CN)$_2$/TiO$_2$ measured at 488 nm in the presence (dashed lines) and absence (solid lines) of 0.5 M NaI in propylene carbonate electrolyte. The transients represent an average of 10 traces. The samples were excited with 532-nm light (8−10 ns fwhm, 6 mJ/pulse).

The kinetic data are summarized in Table 1 for consecutive measurements on a series of five different sensitized electrodes prepared from the same batch of sol−gel processed TiO$_2$.

Discussion

The photoelectrochemical properties of the sensitizers anchored to DeGussa or sol−gel processed TiO$_2$ films in propylene carbonate or acetonitrile electrolyte reveal that *cis*-Ru(dcb)$_2$(CN)$_2$/TiO$_2$ converts photons into electrons more efficiently than does *cis*-Os(dcb)$_2$(CN)$_2$/TiO$_2$. This finding is consistent with our previous studies using the so-called "fractal" TiO$_2$ films sensitized with these same compounds.[5] When corrections are made for ground-state absorption, reflection, and competitive light absorption by the tin oxide support, the photon-to-current efficiency of *cis*-Ru(dcb)$_2$(CN)$_2$/TiO$_2$ approaches unity at single wavelengths of light and is therefore one of the most efficient sensitizers identified to date.[5,9] The fact that very similar behavior is observed on different TiO$_2$ materials and in aqueous and nonaqueous electrolytes strongly suggests that the lower photocurrent efficiency from *cis*-Os(dcb)$_2$(CN)$_2$ stems mainly from the molecular sensitizer and not the TiO$_2$ materials or electrolytes.

Transient absorption and reflectance measurements after selective excitation of the molecular sensitizer allow the interfacial charge separation, recombination, and regeneration processes to be monitored, k_2, k_3, and k_4, respectively, Scheme 1. The nanosecond data reported here fail to time resolve the interfacial charge separation process as expected, $k_2 > 7 \times 10^7$ s^{-1}.[7] In contrast, recombination of the electron in the solid with the oxidized sensitizer occurs on a microsecond time scale for both these sensitizers. Assuming a common donor in TiO$_2$ and that redox potentials measured in fluid solution translate to the interface, the thermodynamic driving force for interfacial charge recombination, k_3, is expected to be 340 mV larger for [Ru^{III}(dcb)$_2$(CN)$_2$]$^+$ than for [Os^{III}(dcb)$_2$(CN)$_2$]$^+$. The fact that the transients observed are within experimental error the same for both sensitizers indicates that the recombination process is either

insensitive to this driving force change or that the difference in rate cannot be resolved under our experimental conditions. In either case, the data provides no clear evidence that k_3 falls in the Marcus inverted region as was previously suggested.[5]

Diffuse reflectance measurements in the presence of 0.5 M NaI demonstrate quite conclusively that the halide oxidation rate is sluggish after light excitation of *cis*-Os(dcb)$_2$(CN)$_2$/TiO$_2$. Slow iodide oxidation by Os^{III}(dcb)$_2$(CN)$_2^+$/TiO$_2$ allows efficient recombination with e$^-$(TiO$_2$) instead, thereby wasting the transiently stored energy. Iodide oxidation, therefore, is the rate-limiting step in the sensitization of a nanocrystalline TiO$_2$ particle by *cis*-Os(dcb)$_2$(CN)$_2$. For Ru^{III}(dcb)$_2$(CN)$_2^+$/TiO$_2$, on the other hand, iodide efficiently intercepts the interfacial charge-separated state and regenerates the sensitizer ground state within about 200 ns. Therefore, efficient photocurrents are realized in regenerative solar cells.

The outer-sphere one-electron oxidation of iodide by transition metal coordination complexes have been well studied and are the subject of a recent review.[13] The expected stoichiometric reaction is given in eq 3. For strong oxidants only the forward

$$2M_{ox} + 2I^- \rightleftharpoons 2M_{red} + I_2 \quad (3)$$

reaction needs to be considered while for weaker oxidants, such as Os(bpy)$_3$3+, both forward and reverse reactions need to be taken into consideration.[14] Equation 3 masks a much more complex reaction mechanism. Outer-sphere iodide oxidation by transition metal complexes is known to follow two parallel paths in aqueous solution, eqs 4 and 5.[14] Both reactions are first order in transition metal complex, but are first and second order in iodide, respectively.

$$M^{III}(dcb)_2(CN)_2^+ + I^- \rightarrow M^{II}(dcb)_2(CN)_2 + I^\bullet \quad (4)$$

$$M^{III}(dcb)_2(CN)_2^+ + 2I^- \rightarrow M^{II}(dcb)_2(CN)_2 + I_2^{-\bullet} \quad (5)$$

Proposed mechanisms for eq 5 include I$^-$ reacting with an [M$_{ox}$,I$^-$] ion pair or M$_{ox}$ with an [I$^-$,I$^-$] ion pair.[14] The iodide reduction potentials remain unknown in nonaqueous solutions but have been determined in water, $E°(I/I^-) = 1.33$ V and $E°(2I^-/I_2^-.) = 0.94$ V.[15] The measured sensitizer reduction potentials predict that iodide oxidation is thermodynamically uphill by either pathway in aqueous solution. However, we qualitatively expect more facile iodide oxidation in organic electrolyte solutions based on the more favorable solvation of iodide by water and the iodine atom and I$_2^-$ by organic solvents. Furthermore, surface adsorption, ion pairing, and the nature of the cation may all effect these potentials in an unknown manner.[16,17] Nevertheless, iodide oxidation by Os^{III}(dcb)$_2$(CN)$_2^+$/TiO$_2$ should be thermodynamically less favorable than oxidation by Ru^{III}(dcb)$_2$(CN)$_2^+$/TiO$_2$ in agreement with the kinetic data reported here.

Conclusion

In regenerative photoelectrochemical cells *cis*-Ru(dcb)$_2$(CN)$_2$ anchored to nanocrystalline TiO$_2$ converts photons to electrons quantitatively while the analogous Os(II) sensitizer does not. Time-resolved absorbance and reflectance measurements demonstrate that the lower photocurrent efficiency is due to a sluggish iodide oxidation rate by *cis*-Os^{III}(dcb)$_2$(CN)$_2^+$/TiO$_2$. Iodide oxidation, therefore, is the rate-limiting step in the sensitization of nanocrystalline TiO$_2$ with this sensitizer in acetonitrile or propylene carbonate electrolytes. Photoelectrochemical measurements alone did not allow this conclusion to be drawn. In fact, photoelectrochemistry generally does not provide molecular insights into why one sensitizer performs more efficiently than another. Transient diffuse reflectance and absorption measurements, on the other hand, do provide quantitative insights and represent simple in situ techniques for sensitizer evaluation.

To achieve high photocurrent production with Os(II) polypyridyl sensitizers, alternative strategies must be adopted to enhance donor oxidation efficiencies. Stronger reducing agents as electrolyte donors or sensitizers with more positive Os$^{III/II}$ reduction potentials should produce higher photocurrents. The former strategy can be accomplished by tuning the iodide oxidation potential through ion-pairing[16] and solution modification,[17] for example, or by using alternative donors.[18] The latter strategy can be realized with strong, nonchromophoric, π-acceptor ligands such as CO or isocyanides. Studies of this type, directed toward efficient semiconductor sensitization by Os(II) transition metal complexes, are currently underway in our laboratories.

Acknowledgment. G.J.M. acknowledges the Division of Chemical Sciences, Office of Basic Energy Sciences, Office of Energy Research, U.S. Department of Energy for research support. C.A.B. acknowledges EU for financial support under the Joule III program, Contract No. JOR3CT960107. T.A.H. acknowledges support from a Sonneborn fellowship. NATO (CRG 960735) is acknowledged for travel support.

Supporting Information Available: Diffuse reflectance transients for (a) *cis*-Ru(dcb)$_2$(CN)$_2$/TiO$_2$ and (b) *cis*-Os(dcb)$_2$(CN)$_2$/TiO$_2$ (2 pages). See any current masthead page for ordering information and Web access instructions.

References and Notes

(1) (a) Fox, M. A.; Chanon, M. *Photoinduced Electron Transfer*; Elsevier: Amsterdam, 1988. (b) Gratzel, M. *Heterogeneous Photochemical Electron Transfer*; CRC: Boca Raton, 1989.

(2) O'Regan, B.; Grätzel, M. *Nature* **1991**, *353*, 737.

(3) Hagfeldt, A.; Grätzel, M. *Chem. Rev.* **1995**, *95*, 49.

(4) Stipkala, J. M.; Castellano, F. N.; Heimer, T. A.; Kelly, C. A.; Livi, K. J. T.; Meyer, G. J. *Chem. Mater.* **1997**, *9*, 2341, and references therein.

(5) Heimer, T. A.; Bignozzi, C. A.; Meyer, G. J. *J. Phys. Chem.* **1993**, *97*, 11987.

(6) Kalyanasundaram, K. *Photochemistry of Polypyridine and Porphyrin Complexes;* Academic Press: New York, 1992.

(7) (a) Tachibana, Y.; Moser, J. E.; Grätzel, M.; Klug, D. R.; Durrant, J. *J. Phys. Chem.* **1996**, *100*, 20056. (b) Heimer, T. A.; Meyer, G. J. *J. Lumin.* **1996**, *70*, 468. (c) Hannappel, T.; Burfeindt, B.; Storck, W.; Willig, F. *J. Phys. Chem. B* **1997**, *101*, 6799. (d) Heimer, T. A.; Heilweil, E. J. *J. Phys. Chem. B* **1997**, *101*, 10990.

(8) Heimer, T. A.; Meyer, G. J. *Proc. Electrochem. Soc.* **1994**, *95*−*98*, 167.

(9) (a) Argazzi, R.; Bignozzi, C. A.; Heimer, T. A.; Castellano, F. N.; Meyer, G. J. *Inorg. Chem.* **1994**, *33*, 5741. (b) Nazeeruddin, M. K.; Kay, A.; Rodicio, I.; Humphry-Baker, R.; Muller, E.; Liska, P.; Vlachopoulos, N.; Grätzel, M. *J. Am. Chem. Soc.* **1993**, *115*, 6382.

(10) Heimer, T. A.; D'Arcangelis, S. T.; Farzad, F.; Stipkala, J. M.; Meyer, G. J. *Inorg. Chem.* **1996**, *35*, 5319.

(11) (a) Wendlandt, W. W.; Hecht, G. G. *Reflectance Spectroscopy;* Interscience: New York, 1966; p 46. (b) Kessler, R. W.; Wilkinson, F. *J. Chem. Soc., Faraday Trans. 1* **1981**, *77*, 309.

(12) Draper, R. B.; Fox, M. A. *J. Phys. Chem.* **1990**, *94*, 4628.

(13) Nord, G. *Comments Inorg. Chem.* **1992**, *13*, 221.

(14) (a) Nord, G.; Pedersen, B.; Farver, O. *Inorg. Chem.* **1978**, *17*, 2233. (b) Nord, G.; Pedersen, B.; Floryan-Lovberg, E.; Pagsberg, P. *Inorg. Chem.* **1982**, *21*, 2327.

(15) Stanbury, D. M. *Adv. Inorg. Chem.* **1989**, *33*, 69.

(16) Fitzmaurice, D.; Frei, H. *Langmuir* **1991**, *7*, 1129.

(17) Myung, N.; Licht, S. *J. Electrochem. Soc.* **1995**, *142*, L129.

(18) Argazzi, R.; Bignozzi, C. A.; Heimer, T. A.; Castellano, F. N.; Meyer, G. J. *J. Phys. Chem. B* **1997**, *101*, 2591.